

# Quantum receiver for quadrature phase-shift keying at the single photon level

Jasminder S. Sidhu,<sup>1,2,\*</sup> Shuro Izumi,<sup>3</sup> Jonas S. Neergaard-Nielsen,<sup>3</sup> Cosmo Lupo,<sup>2,†</sup> and Ulrik L. Andersen<sup>3</sup>

<sup>1</sup>*SUPA Department of Physics, The University of Strathclyde, Glasgow, G4 0NG, UK*

<sup>2</sup>*Department of Physics and Astronomy, The University of Sheffield, Sheffield, S3 7RH, UK*

<sup>3</sup>*Center for Macroscopic Quantum States (bigQ), Department of Physics,  
Technical University of Denmark, Fysikvej, 2800 Kgs. Lyngby, Denmark*

(Dated: June 13, 2022)

Quantum enhanced receivers are endowed with resources to achieve higher sensitivities than conventional technologies. For application in optical communications, they provide improved discriminatory capabilities for multiple non-orthogonal quantum states. In this work, we propose and experimentally demonstrate a new decoding scheme for quadrature phase-shift encoded signals. Our receiver surpasses the standard quantum limit and outperforms all previously known non-adaptive detectors at low input powers. Unlike existing approaches, our receiver only exploits auxiliary coherent-state fields, linear optics, and on-off photo-detection. This circumvents the requirement for challenging feed-forward operations that limit communication transmission rates and can be readily implemented with current technology.

## I. INTRODUCTION

Quantum mechanics places strict fundamental limits on our ability to discriminate non-orthogonal quantum states [1, 2]. This is a deep-rooted property of quantum mechanics which, on one hand, fuels numerous applications in quantum information science such as quantum computing and quantum key distribution [3–5], and on the other, limits the performance of other protocols such as sensing, metrology [6–8] and communication. The mathematical framework around state discrimination is based on the theory of quantum detection [1], and it has been applied to study the discrimination of various quantum states [9–11].

Of particular importance is the efficient discrimination of weak coherent states. Coherent states are endowed with an intrinsic resilience to loss and, given their immediate availability, have become indispensable information carriers in the optical realisation of classical [12] and quantum information protocols [13, 14]. An alphabet of coherent states with very small amplitudes (down to the single photon level) possesses large state overlaps, and thus exhibits strong quantum features. Such a small-amplitude alphabet occurs often in quantum communication protocols and in classical communication schemes that aim to enhance channel capacities [15]. More specifically, the optimal discrimination of weak coherent states can be used to enhance the secure key rate in quantum key distribution, improve the success rate in entanglement distillation and increase the distance of deep-space communication [16, 17].

This work focuses on the discrimination of four weak coherent states with equal amplitude and equidistant phase separations,  $\{|a\rangle, |ia\rangle, |-\alpha\rangle, |-ia\rangle\}$ , chosen with equal prior probabilities, where the amplitude  $\alpha$  is real-valued and positive. This ensemble is referred to as quadrature phase shift keying (QPSK) and is commonplace in fibre networks [18]. It offers efficient encoding of two bits of information in one mode of the electromagnetic field. Efficient readout of the encoded infor-

mation can be accomplished by measuring conjugate quadratures via a heterodyne detection [12, 19]. However, the optimal bound on the discrimination error (that is, the minimum average error in discriminating QPSK coherent states), known as the Helstrom bound, is significantly lower than that attainable through heterodyne detection [20, 21]. A practical setup for discriminating the QPSK coherent states at the exact Helstrom limit is unknown. However, it is possible to surpass the heterodyne limit and approach the Helstrom bound using different decoding strategies. These schemes generally use a combination of linear optics, photo-detection, and globally optimised displacement operations to distinguish coherent states through conditional signal nulling. Specifically, in the regime of large signal amplitudes ( $\alpha \gtrsim 2$ ) the average error probability can be decreased by adaptively updating the displacement phase [22–27]. Moreover, by optimising displacement amplitudes, it is possible to outperform the heterodyne detection limit for any signal amplitude [28, 29]. Alternative sub-optimal receivers use hybrid strategies that combine homodyne detection with adaptive displacements followed by photodetection to beat the heterodyne detection limit for all signal amplitudes [30, 31].

While receivers based on adaptive feedback indeed exhibit superior performance, e.g. outperforming the heterodyne detection limit for all amplitudes, they are technically challenging to implement and their bandwidth is intrinsically limited by the feedback mechanism. It is therefore essential to devise a detection system that beats the heterodyne detection limit without the use of feedback techniques [32]. It has been shown that for large coherent state amplitudes ( $\alpha \gtrsim 2$ ), this is possible by solely using linear optics and photo-detection without the adoption of feedback [23, 33]. However, displaying the same advantage for weak coherent states still remains an open question.

In this paper, we introduce, characterise, and experimentally demonstrate a new decoding strategy for QPSK states, comprised of multi-mode linear optics, ancillary coherent states, and photo-detection. Notably, we do not make use of adaptive measurements, feed-forward, or photon number resolution. We show that adaptive feedback is not necessary to beat the conventional heterodyne decoding limit in the fully quantum, weak coherent amplitude regime ( $\alpha \lesssim 0.5$ ). We experimen-

\*Electronic address: [jsmdrsidhu@gmail.com](mailto:jsmdrsidhu@gmail.com)

†Electronic address: [c.lupo@sheffield.ac.uk](mailto:c.lupo@sheffield.ac.uk)

tally realise the receiver and evidence strong agreement with theoretical predictions that account for the system efficiency. This work demonstrates a fundamental advance towards sub-optimal optical receivers, and provides an immediate, practical strategy to surpass the heterodyne detection limit with currently available technology. Our strategy is compatible with photon number resolving detection that can increase the robustness of the receiver against noise and extend the performance of our scheme to higher input intensities [24, 26, 34].

The theoretical framework of this paper is presented in Section II. In Section III, we present our new receiver for QPSK decoding. We demonstrate that our receiver outperforms all previous decoding strategies in the weak amplitude regime, and present an experimental demonstration of this in Section IV. Conclusions are summarised in Section V.

## II. THEORETICAL FRAMEWORK

Consider the problem of identifying a quantum state  $\rho$  drawn from a known finite set  $\{\rho_1, \rho_2, \dots, \rho_n\}$  with prior probabilities  $\{p_1, p_2, \dots, p_n\}$  [4, 35]. We focus on a single-shot scenario where only a single instance of the state is available. When the states  $\rho_x$  are mutually orthogonal, detectors placed along the orthogonal directions will be able to perform perfect state discrimination. However, perfect discrimination of non-orthogonal states is not possible from a single-shot experiment and finding an optimal optical receiver is generally a difficult task. We consider this problem within the framework of ambiguous state discrimination, i.e., we account for a finite probability of error that we aim to minimise.

Consider a general scheme for structured detection where the unknown state  $\rho$  is mixed with a known ancillary state  $\sigma$  through a unitary transformation  $U$ . The two output systems are then measured by applying a given measurement  $M$ , which is characterised by the POVM elements  $M_y$ , with  $y = \{1, \dots, m\}$ . This is shown schematically in the inset of Fig. 1. While the measurement is fixed, the ancillary state  $\sigma$  and the unitary  $U$  can be chosen within given sets, respectively denoted as  $\mathcal{S}$  and  $\mathcal{U}$ . This model applies to any number of arbitrary quantum states.

For applications in quantum optics, coherent state discrimination represents a concrete example of this general quantum state discrimination problem. We consider a setup where the unknown state  $\rho$  is a coherent state over  $s$  optical modes,  $\sigma$  is a known coherent state over  $t$  modes, and the measurement  $M$  is a mode-wise photon detection, as shown in Fig. 1. By using passive linear optical transformations, the unitary  $U$  is chosen from the set of multimode transformations that are realised from a combination of beam splitters (BS) and phase shifters. This decomposition holds for any passive linear optics over a finite number of optical modes [36, 37].

We now determine the optimal unitary  $U$  and ancilla  $\sigma$  that maximise the average probability of successful discrimination. For given  $\rho_x$ ,  $U$ , and  $\sigma$ , we directly compute the probability of obtaining the measurement outcome  $y$  as

$$p_{U,\sigma}(y|x) = \text{Tr} \left[ \left( U \rho_x \otimes \sigma U^\dagger \right) M_y \right]. \quad (1)$$

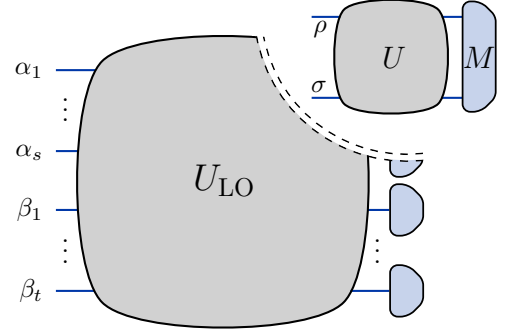


FIG. 1: Inset: a general ancilla-assisted discrimination scheme, with  $\rho$  an unknown state,  $\sigma$  a known ancillary state,  $U$  is a unitary transformation, and  $M$  a measurement. An application of this general scheme to discriminate multiple coherent states is shown using only passive linear optics and photon detection. The input ensemble is made of  $s$ -mode coherent states of unknown amplitudes. The scheme uses  $t$  ancillary modes prepared in coherent states of known amplitudes. The final measurement is realised as  $s + t$  independent photon detectors.

By applying the Bayes rule and the principle of maximum likelihood, our best guess for  $x$ , given the measurement output  $y$ , is  $\hat{x}$  such that

$$p_{U,\sigma}(\hat{x}|y) = \max_x p_{U,\sigma}(x|y), \quad (2)$$

where  $p_{U,\sigma}(\hat{x}|y)$  is the probability of successfully identifying the input state given the output measurement  $y$ . The average success probability is then given by

$$p_{U,\sigma} = \sum_y p_{U,\sigma}(y) \max_x p_{U,\sigma}(x|y) \quad (3)$$

$$= \sum_y p_{U,\sigma}(y) \max_x \frac{p_{U,\sigma}(y|x)p(x)}{p_{U,\sigma}(y)} \quad (4)$$

$$= \sum_y \max_x p_{U,\sigma}(y|x)p(x), \quad (5)$$

where in Eq. (4) we have applied the Bayes rule.

The optimisation routine consists in finding the ancillary state  $\sigma \in \mathcal{S}$  and the unitary  $U \in \mathcal{U}$  that maximise  $p_{U,\sigma}$ . This yields the optimised success probability

$$p_s = \sup_{U \in \mathcal{U}, \sigma \in \mathcal{S}} p_{U,\sigma}. \quad (6)$$

Note that this quantity is a function of the sets  $\mathcal{U}$  and  $\mathcal{S}$  only, in addition to the input ensemble and measurement  $M$ . In the following section, we apply this approach to the problem of discriminating a quaternary coherent state alphabet. Our decoder is optimal under the condition that  $U$  represents a passive linear optical transformation, with auxiliary coherent states and photon detection.

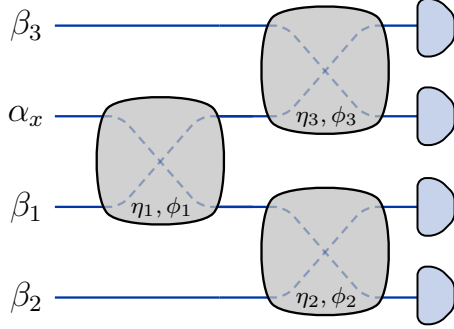


FIG. 2: A scheme for discrimination of QPSK with three auxiliary coherent states. The passive linear optics unitary consists of three beam splitters.

### III. QUADRATURE PHASE-SHIFT KEYING

In QPSK, the unknown states are coherent states,  $\rho_x \equiv |\alpha_x\rangle = |i^x \alpha\rangle$ , with  $x \in \{0, 1, 2, 3\}$ , and  $\alpha > 0$  [18]. A practical measurement scheme to distinguish between these states is heterodyne detection, which, in average, is successful with probability

$$p_{\text{het}} = \frac{1}{4} \left( 1 + \text{erf} \left[ \frac{\alpha}{\sqrt{2}} \right] \right)^2. \quad (7)$$

To apply our general detection scheme to QPSK, we first fix the number of ancillary modes. This generally depends on the properties of the states to distinguish. A general passive linear optical transformation is then implemented following the recipe of Reck, Zeilinger, Bernstein, and Bertani (RZBB) [36]. Here, any passive linear transformation on  $N$  input modes can be uniquely decomposed into  $N(N - 1)/2$  BSs with suitable phase shifters. Each BS is characterised by its transmissivity  $\eta$  and phase  $\phi$ , and transforms a pair of input coherent states with amplitudes  $\alpha, \beta$  into

$$\alpha' = \sqrt{\eta} \alpha + e^{i\phi} \sqrt{1 - \eta} \beta, \quad \beta' = \sqrt{1 - \eta} \alpha - e^{i\phi} \sqrt{\eta} \beta. \quad (8)$$

Together with the amplitudes of the ancillary states, we collectively refer to these parameters as the optimisation parameters. By optimising the success probability in Eq. (6) over all optimisation parameters, we determine the optimal QPSK receiver. In the following, we focus on the regime of weak signals,  $\alpha \lesssim 0.5$ .

We first consider three ancillary states in addition to a dedicated QPSK input to the transformation matrix (i.e.,  $N = 4$ ). Under the fully general RZBB scheme [36], this amounts to optimising over six BSs and three ancillary coherent states with amplitudes  $\beta_1, \beta_2, \beta_3$ . A simpler scheme on four input modes is the architecture of three BSs illustrated in Fig. 2. A numerical optimisation yields the same success probability for both these schemes. For both schemes, the optimal values of the parameters depend on the coherent state amplitude.

A numerical search indicates a simpler but still optimal receiver that utilises a single ancilla state as shown in Fig. 3a. Recall that a displacement operation  $D(b)$  is implemented by

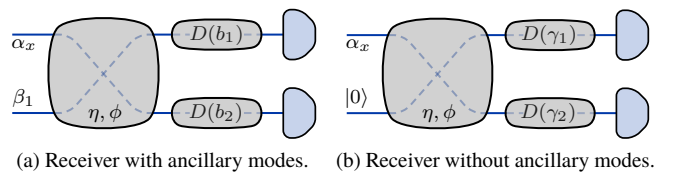


FIG. 3: An optimal receiver for QPSK discrimination. Fig. 3a: The unknown coherent state is first mixed with an auxiliary coherent state  $\beta_1$  at a BS with transmissivity  $\eta$  and phase  $\phi$ . Each mode is then independently displaced in phase space by with  $b_1, b_2$ , before being detected using bucket detectors. Fig. 3b illustrates an equivalent receiver but without an ancillary mode. This simply requires updating the displacements  $D(b_j) \rightarrow D(\gamma_j)$  and is easier to implement.

mixing the signal with a bright coherent state at a highly transmissive BS [38]. Therefore, the second and third BSs in Fig. 2 can be replaced by displacement operators as illustrated in Fig. 3a. The displacement  $D(b)$  maps a coherent state of amplitude  $\alpha$  into  $\alpha' = \alpha + b$ . Including displacement parameters, this scheme corresponds to an optimisation problem that comprises eight parameters in total, the result of which depends on the coherent state amplitudes  $\alpha$ . Notice that this maximises the sum of the individual success probabilities. This is more general than the conventional nulling strategy, which though de-exciting a signal to vacuum, only maximises the success probability of the nulled signal.

We also find an analytical solution that is an excellent approximation of the numerical optimal in the regime of weak amplitudes. Furthermore, this solution does not require each parameter to be tuned to specific values of  $\alpha$ . This near optimal receiver is attained through the following parameters:

$$\beta_1 = \frac{1}{\sqrt{2}}, \eta = \frac{1}{2}, \phi = 0, b_1 = b_2 = \frac{i}{2}. \quad (9)$$

With this, the computational overheads are greatly reduced, and an experimental implementation to discriminate QPSK states below the standard quantum limit can be easily performed for weak signal amplitudes. For this near optimal choice of parameters, we obtain the following analytical expression for the average success probability (see Appendix A for proof):

$$p_s = \frac{1}{4} \left( 1 + 2 \exp \left[ -\frac{1 + \alpha^2}{2} \right] \sinh \left[ \frac{\alpha}{\sqrt{2}} \right] \right)^2. \quad (10)$$

We further simplify our optimal QPSK decoder by removing the need for auxiliary coherent states. Notice that an auxiliary coherent state with amplitude  $\beta$  preceding a BS can equivalently be replaced by displacement operations  $D(\sqrt{\eta}\beta), D(-\sqrt{1 - \eta}\beta)$  on modes 1 and 2 respectively after the BS. This is illustrated in Fig. 3b. For the near optimal parameters provided above, the complex displacements required are defined through  $\gamma_1 = b_1 + 1/2, \gamma_2 = b_2 - 1/2$ .

We benchmark the success probability of our optimal receiver scheme with the Helstrom bound and heterodyne detection in Fig. 4. Our scheme outperforms both heterodyne

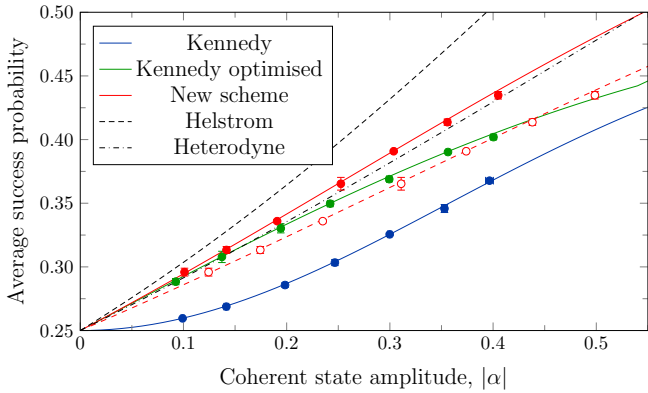


FIG. 4: Average success probability of distinguishing QPSK coherent states as a function of the signal amplitude  $\alpha$  for different receivers. The theoretical success probability of our scheme (Eq. (10)) is shown in solid red. Heterodyne (from Eq. (7)) is shown in dashed-dotted black, and the Helstrom bound [21] in dashed grey. The filled red circles represent experimental results adjusted to correct the experimental 66% efficiency (empty circles are the un-adjusted experimental data). The blue solid line and filled circles are for a conventional nulling Kennedy receiver [40]. Green solid lines and filled circles are for the Kennedy receiver with optimised displacement amplitudes [41].

detection and Müller's hybrid scheme [31] in the small amplitude regime. Unlike Müller's receiver, our scheme is implemented using only linear optics and photon counting and does not rely on adaptive conditioning of the optimisation parameters. In searching for an optimal receiver setup, here we have focused on the small-amplitude regime. Therefore, it comes with no surprise that heterodyne measurement outperforms our scheme for larger amplitudes. Furthermore, the performance lost is also related to the fact that on-off detectors cannot efficiently extract multi-photon information. The use of photon number resolving detection may help to extend the relative performance improvement of our scheme in addition to providing robustness under realistic conditions at high intensities [26, 39].

#### IV. EXPERIMENTAL DEMONSTRATION

We experimentally demonstrate our QPSK decoder in the temporal mode representation, where the displacement operation is successively changed in time [42]. This allows us to detect two optical modes using only one detector.

Our experimental setup is shown in Fig. 5. We use a continuous wave laser at 1550 nm, which is split into two optical paths in order to individually prepare the signal coherent state and the auxiliary coherent state for the displacement operation. A variable attenuator and a piezo transducer respectively control the amplitude and the phase of the signal state. A phase modulator on the auxiliary coherent state path controls the phase of the displacement operation with a maximum frequency of 1 MHz. Since the temporal width of the signal state is defined to be 100  $\mu$ s, the displacement phase can be

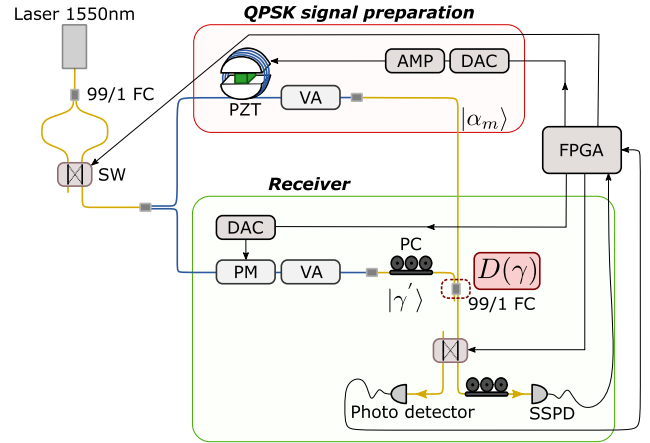


FIG. 5: Experimental setup. FC: fiber coupler, SW: optical switch, PM: phase modulator, PZT: piezo transducer, VA: variable attenuator, PC: polarisation controller, SSPD: superconducting nanowire single photon detector, DAC: digital to analog converter, AMP: amplifier.

changed to the desired condition with little adversary effect from the finite bandwidth of the phase modulation. The signal state is combined with the auxiliary state at the 99/1 fiber coupler corresponding to the physical implementation of the displacement operation. Using an optical switch, the interfered beam is guided to either a photo detector for the purpose of stabilising the relative phase between signal and auxiliary states, or a superconducting nanowire single photon detector (SSPD) for data acquisition. Because the conventional photon detector cannot measure the laser power highly attenuated to photon level, the laser power is also switched between high and low by an optical switch after the laser source. A field programmable gate array (FPGA) collects the electrical signals from the SSPD and generates the signal driving the phase modulator. We achieve a total system efficiency of about 66%, where the transmission efficiency from before the 99/1 fiber coupler to the SSPD is approximately 90%. The detection efficiency of the SSPD is measured to be approximately 73% and the dark count noise around 25 Hz [27].

We experimentally investigate the performance of three types of two-mode receivers based on displacement operations and photon detections. The three schemes are illustrated on phase space diagrams in Fig. 6 and the experimentally obtained performances of the receivers are depicted in Fig. 4. Blue solid line and filled circles are the success probabilities for theoretical predictions and experimental results for a conventional nulling Kennedy receiver which implements the displacement operations such that one of the QPSK signals is displaced to the vacuum state, i.e.  $|\gamma_1| = |\gamma_2| = |\alpha|/\sqrt{2}$  with  $\eta = 1/2$  [40] (Fig. 6(a)). The mean and error bars of the success probabilities are evaluated from five independent procedures with  $4 \times 10^4$  data points for each procedure, and the signal amplitude is calibrated from the observed photon count rate by blocking the auxiliary state path. Green solid lines and filled circles are for the Kennedy receiver with optimised displacement ampli-

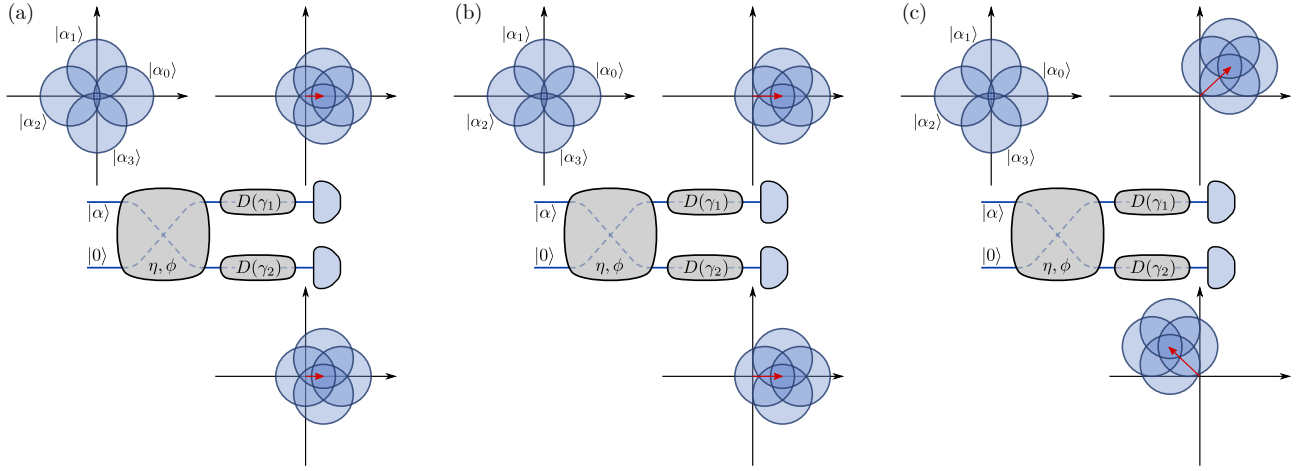


FIG. 6: Illustration of the three receiver schemes implemented in the experiment for discriminating between the four input QPSK states  $|\alpha_0\rangle, |\alpha_1\rangle, |\alpha_2\rangle, |\alpha_3\rangle$ . (a) In the nulling Kennedy receiver [40], both BS outputs are displaced such that the  $|\alpha_2\rangle$  state is shifted to the phase space origin. (b) The amplitude-optimised Kennedy receiver [41] is similar to the nulling receiver, but by displacing  $|\alpha_2\rangle$  further past the origin, the success probabilities for weak amplitudes are significantly improved. (c) Our optimal receiver also optimises the phases of the displacements on the two BS outputs, leading to further improvements.

tude [41] (Fig. 6(b)). Our numerical analysis indicates that, for both nulling and displacement amplitude optimised receivers, the displacement phases for modes 1 and 2 should be set to the same value to maximise the average success probability in the very weak amplitude case. For the displacement amplitude optimised receiver, the near optimal performance for the weak coherent signal amplitude is obtained with  $|\gamma_1| = |\gamma_2| = 1/2$  and  $\eta = 1/2$ . The conventional approaches are unable to beat the heterodyne limit, given by the black dash-dotted line, in the weak coherent amplitude range. On the other hand, as shown by red solid line and filled circles, our strategy of optimising the phase of the displacement operations (Fig. 6(c)), implemented with the near optimal parameters, provides an improved performance that overcomes the heterodyne limit. Since our system has the finite detection efficiency of 66%, the success probability is degraded and the performances in the actual experimental condition are plotted for the optimal receiver by a dashed curve and open circles for theory and experiment, respectively.

## V. CONCLUSIONS

Non-orthogonal quantum states are the building blocks of quantum communication protocols. Weak coherent states are commonly used in these applications given their non-orthogonality, relative ease of generation in laboratories, and resilience to loss. Motivated by this, we have looked at designing practical receivers to discriminate coherent states. In particular, we have focused on the optimal receivers that can be obtained by combining linear optics, ancillary coherent states of known amplitude, and on-off photo-detectors.

The natural decoders for discriminating coherent states are homodyne and heterodyne detections. These detectors have

the advantage of being already commonly employed in standard telecommunications. However, they are limited by the shot noise. Several works have focused on the design of structured receiver that could beat the shot noise limit. In particular, for the problem of decoding QPSK, the only known sub-shot-noise strategies in the low amplitude regime exploit feed-forward [28, 29, 31]. Although feasible in principle, approaches based on feed-forward remain technically demanding.

Here, we develop a novel sub-shot-noise QPSK decoding. Our scheme employs linear optics, coherent state ancillas, and on-off photo-detectors, without feed-forward operations. We demonstrate that it outperforms heterodyne detection, as well as all previous non-adaptive detectors in the weak pulse regime. Experimental implementation of our novel receiver demonstrates results consistent with our theoretical analysis.

An interesting experimental platform to test some of this work is the hybrid spatio-temporal architecture for universal linear optics [43]. This scheme would be useful to implement the optimised unitary receivers that we construct based on the design by Reck, Zeilinger, Bernstein, and Bertani [36]. It would be interesting to see how this proposal compares with the experimental minimum error measurements proposed by Solís-Prosser *et al.* [2].

Our results pave the way to a number of research questions. First of all, as here we have focused on the regime of weak coherent states ( $\alpha \lesssim 0.5$ ), this leaves open the problem of finding optimal linear-optics receivers for larger amplitudes. Photon number resolving detectors may further improve our decoding strategy, especially in the region of higher signal amplitudes. Alternatively, splitting the signal in more optical modes can also improve the discrimination efficiency at higher amplitudes [23]. Our approach may be optimal for the discrimination of higher-order constellations of coherent states, beyond QPSK.

Finally, it may be combined with error correcting codes and exploited to demonstrate the phenomenon of super-additivity in unambiguous coherent state discrimination.

## VI. ACKNOWLEDGEMENTS

JSS and CL acknowledge EPSRC for funding via the Quantum Communications Hub (EP/M013472/1). SI, JSNN and

ULA acknowledge the Danish National Research Foundation through the Center for Macroscopic Quantum States (DNRF142). We would like to thank Masahiro Takeoka and Saikat Guha for useful discussions on an earlier version of the manuscript and T. Yamashita, S. Miki, and H. Terai for providing and installing the superconducting nanowire single photon detector.

---

[1] C. W. Helstrom, “Detection theory and quantum mechanics,” *Inform. Control*, vol. 10, no. 3, pp. 254–291, 1967.

[2] M. A. Solís-Prosser, M. F. Fernandes, O. Jiménez, A. Delgado, and L. Neves, “Experimental minimum-error quantum-state discrimination in high dimensions,” *Phys. Rev. Lett.*, vol. 118, p. 100501, March 2017.

[3] C. H. Bennett, “Quantum cryptography using any two nonorthogonal states,” *Phys. Rev. Lett.*, vol. 68, pp. 3121–3124, May 1992.

[4] S. M. Barnett and S. Croke, “Quantum state discrimination,” *Adv. Opt. Photon.*, vol. 1, pp. 238–278, April 2009.

[5] C. H. Bennett and G. Brassard, “Quantum cryptography: Public key distribution and coin tossing,” *Theor. Comput. Sci.*, vol. 560, pp. 7–11, 2014.

[6] M. Ban, K. Kurokawa, R. Momose, and O. Hirota, “Optimum measurements for discrimination among symmetric quantum states and parameter estimation,” *Int. J. Theor. Phys.*, vol. 36, pp. 1269–1288, June 1997.

[7] A. N. Jordan, J. Tollaksen, J. E. Troupe, J. Dressel, and Y. Aharonov, “Heisenberg scaling with weak measurement: a quantum state discrimination point of view,” *Quant Stud: Math and Foundations*, vol. 2, no. 1, pp. 5–15, 2015.

[8] J. S. Sidhu and P. Kok, “Geometric perspective on quantum parameter estimation,” *AVS Quantum Science*, vol. 2, p. 014701, February 2020.

[9] Y. C. Eldar and G. D. Forney, “On quantum detection and the square-root measurement,” *IEEE Trans. Inf. Theory*, vol. 47, pp. 858–872, March 2001.

[10] C.-L. Chou and L. Y. Hsu, “Minimum-error discrimination between symmetric mixed quantum states,” *Phys. Rev. A*, vol. 68, p. 042305, October 2003.

[11] Y. C. Eldar, A. Megretski, and G. C. Verghese, “Optimal detection of symmetric mixed quantum states,” *IEEE Trans. Inf. Theory*, vol. 50, pp. 1198–1207, June 2004.

[12] K. Kikuchi, “Fundamentals of coherent optical fiber communications,” *Journal of Lightwave Technology*, vol. 34, no. 1, pp. 157–179, 2016.

[13] T. C. Ralph, A. Gilchrist, G. J. Milburn, W. J. Munro, and S. Glancy, “Quantum computation with optical coherent states,” *Phys. Rev. A*, vol. 68, p. 042319, Oct 2003.

[14] V. Scarani, H. Bechmann-Pasquinucci, N. J. Cerf, M. Dušek, N. Lütkenhaus, and M. Peev, “The security of practical quantum key distribution,” *Rev. Mod. Phys.*, vol. 81, pp. 1301–1350, Sep 2009.

[15] V. Giovannetti, S. Guha, S. Lloyd, L. Maccone, J. H. Shapiro, and H. P. Yuen, “Classical capacity of the lossy bosonic channel: The exact solution,” *Phys. Rev. Lett.*, vol. 92, p. 027902, Jan 2004.

[16] V. W. S. Chan, “Free-space optical communications,” *Journal of Lightwave Technology*, vol. 24, no. 12, pp. 4750–4762, 2006.

[17] H. Kaushal and G. Kaddoum, “Optical communication in space: Challenges and mitigation techniques,” *IEEE Communications Surveys Tutorials*, vol. 19, no. 1, pp. 57–96, 2017.

[18] V. K. Garg and Y.-C. Wang, *Chapter 4 - Modulation and Demodulation Technologies*. Academic Press, 1 ed., 2005.

[19] C. Weedbrook, S. Pirandola, R. García-Patrón, N. J. Cerf, T. C. Ralph, J. H. Shapiro, and S. Lloyd, “Gaussian quantum information,” *Rev. Mod. Phys.*, vol. 84, pp. 621–669, May 2012.

[20] C. W. Helstrom, *Quantum Detection and Estimation Theory*. Academic Press Inc., 1976.

[21] M. Osaki, M. Ban, and O. Hirota, “Derivation and physical interpretation of the optimum detection operators for coherent-state signals,” *Phys. Rev. A*, vol. 54, pp. 1691–1701, August 1996.

[22] R. S. Bondurant, “Near-quantum optimum receivers for the phase-quadrature coherent-state channel,” *Opt. Lett.*, vol. 18, pp. 1896–1898, November 1993.

[23] S. Izumi, M. Takeoka, M. Fujiwara, N. D. Pozza, A. Assalini, K. Ema, and M. Sasaki, “Displacement receiver for phase-shift-keyed coherent states,” *Phys. Rev. A*, vol. 86, p. 042328, October 2012.

[24] S. Izumi, M. Takeoka, K. Ema, and M. Sasaki, “Quantum receivers with squeezing and photon-number-resolving detectors for  $m$ -ary coherent state discrimination,” *Phys. Rev. A*, vol. 87, p. 042328, April 2013.

[25] F. E. Becerra, J. Fan, G. Baumgartner, J. Goldhar, J. T. Kosloski, and A. Migdall, “Experimental demonstration of a receiver beating the standard quantum limit for multiple nonorthogonal state discrimination,” *Nat. Photon.*, vol. 7, no. 2, pp. 147–152, 2013.

[26] F. E. Becerra, J. Fan, and A. Migdall, “Photon number resolution enables quantum receiver for realistic coherent optical communications,” *Nat. Photon.*, vol. 9, pp. 48–53, November 2015.

[27] S. Izumi, J. S. Neergaard-Nielsen, S. Miki, H. Terai, and U. L. Andersen, “Experimental demonstration of a quantum receiver beating the standard quantum limit at telecom wavelength,” *Phys. Rev. Applied*, vol. 13, p. 054015, May 2020.

[28] C. R. Müller and C. Marquardt, “A robust quantum receiver for phase shift keyed signals,” *New J. Phys.*, vol. 17, p. 032003, March 2015.

[29] A. R. Ferdinand, M. T. DiMario, and F. E. Becerra, “Multi-state discrimination below the quantum noise limit at the single-photon level,” *NPJ Quantum Inf.*, vol. 3, no. 1, p. 43, 2017.

[30] M. A. Usuga, C. Müller, C. Wittmann, M. Takeoka, U. L. Andersen, and G. Leuchs, “Four-state discrimination via a homodyne-kennedy hybrid receiver,” in *CLEO/Europe and EQEC 2009 Conference Digest*, 2009.

[31] C. R. Müller, M. A. Usuga, C. Wittmann, M. Takeoka, C. Mar-

quardt, U. L. Andersen, and G. Leuchs, "Quadrature phase shift keying coherent state discrimination via a hybrid receiver," *New J. Phys.*, vol. 14, p. 083009, August 2012.

[32] F. E. Becerra, J. Fan, G. Baumgartner, S. V. Polyakov, J. Goldhar, J. T. Kosloski, and A. Migdall, " $m$ -ary-state phase-shift-keying discrimination below the homodyne limit," *Phys. Rev. A*, vol. 84, p. 062324, December 2011.

[33] M. T. DiMario, E. Carrasco, R. A. Jackson, and F. E. Becerra, "Implementation of a single-shot receiver for quaternary phase-shift keyed coherent states," *J. Opt. Soc. Am. B*, vol. 35, pp. 568–574, Mar 2018.

[34] K. Li, Y. Zuo, and B. Zhu, "Suppressing the errors due to mode mismatch for  $m$ -ary psk quantum receivers using photon-number-resolving detector," *IEEE Photonics Technol. Lett.*, vol. 25, pp. 2182–2184, November 2013.

[35] J. Bae and L.-C. Kwek, "Quantum state discrimination and its applications," *J. Phys. A: Math. Theoret.*, vol. 48, p. 083001, January 2015.

[36] M. Reck, A. Zeilinger, H. J. Bernstein, and P. Bertani, "Experimental realization of any discrete unitary operator," *Phys. Rev. Lett.*, vol. 73, pp. 58–61, July 1994.

[37] W. R. Clements, P. C. Humphreys, B. J. Metcalf, W. S. Kolthammer, and I. A. Walmsley, "Optimal design for universal multiport interferometers," *Optica*, vol. 3, pp. 1460–1465, Dec 2016.

[38] M. G. A. Paris, "Displacement operator by beam splitter," *Phys. Lett. A*, vol. 217, no. 2, pp. 78–80, 1996.

[39] M. T. DiMario and F. E. Becerra, "Robust measurement for the discrimination of binary coherent states," *Phys. Rev. Lett.*, vol. 121, p. 023603, July 2018.

[40] R. S. Kennedy, "Research laboratory of electronics," Quarterly Progress Report No. 108, MIT, 1973, page 219.

[41] C. Wittmann, M. Takeoka, K. N. Cassemiro, M. Sasaki, G. Leuchs, and U. L. Andersen, "Demonstration of near-optimal discrimination of optical coherent states," *Phys. Rev. Lett.*, vol. 101, p. 210501, November 2008.

[42] M. Takeoka and M. Sasaki, "Discrimination of the binary coherent signal: Gaussian-operation limit and simple non-gaussian near-optimal receivers," *Phys. Rev. A*, vol. 78, p. 022320, August 2008.

[43] D. Su, I. Dhand, L. G. Helt, Z. Vernon, and K. Bradler, "Hybrid spatiotemporal architectures for universal linear optics," *Phys. Rev. A*, vol. 99, p. 062301, June 2019.

### Appendix A: Almost optimal discrimination of QPSK

Consider the receiver in Fig. 3, where the BS has 50% transmissivity and zero phase, the ancillary coherent state has amplitude  $\beta_1 = 1/\sqrt{2}$ , and the displacements on both modes are purely imaginary with amplitude  $b_1 = b_2 = i/2$ .

For a given  $x$ , the action of the BS maps the input and ancillary coherent state in two coherent states of amplitudes:

$$\begin{aligned} \gamma_{1,x} &= \frac{1}{\sqrt{2}} e^{ix\pi/2} \alpha + \frac{1}{\sqrt{2}} \beta_1 = \frac{1}{\sqrt{2}} e^{ix\pi/2} \alpha + \frac{1}{2}, \\ \gamma_{2,x} &= \frac{1}{\sqrt{2}} e^{ix\pi/2} \alpha - \frac{1}{\sqrt{2}} \beta_1 = \frac{1}{\sqrt{2}} e^{ix\pi/2} \alpha - \frac{1}{2}. \end{aligned} \quad (\text{A1})$$

The displacement operators further transform the ampli-

tudes into

$$\begin{aligned} & \frac{\alpha}{\sqrt{2}} \exp \left[ \frac{ix\pi}{2} \right] \pm \frac{1}{2} + \frac{i}{2} \\ &= \frac{\alpha}{\sqrt{2}} \left[ \cos \left( \frac{x\pi}{2} \right) + i \sin \left( \frac{x\pi}{2} \right) \right] \pm \frac{1}{2} + \frac{i}{2} \end{aligned} \quad (\text{A2})$$

$$= \left[ \frac{\alpha}{\sqrt{2}} \cos \left( \frac{x\pi}{2} \right) \pm \frac{1}{2} \right] + i \left[ \frac{\alpha}{\sqrt{2}} \sin \left( \frac{x\pi}{2} \right) + \frac{1}{2} \right]. \quad (\text{A3})$$

Defining  $p(y|x)$  as the probability of obtaining the measurement outcome  $y$  given the input state  $\alpha_x$ , then the probability of individual detectors to click is given by

$$p_{\pm}(1|x) = 1 - \exp \left[ -\frac{1+\alpha^2}{2} - \frac{\alpha}{\sqrt{2}} \left\{ \sin \left( \frac{x\pi}{2} \right) \pm \cos \left( \frac{x\pi}{2} \right) \right\} \right]. \quad (\text{A4})$$

In conclusion, we table the detection probability for each input state:

$$x = 0 \rightarrow \begin{cases} p_+(1|0) = 1 - \exp \left[ -\frac{1+\alpha^2+\sqrt{2}\alpha}{2} \right] \\ p_-(1|0) = 1 - \exp \left[ -\frac{1+\alpha^2-\sqrt{2}\alpha}{2} \right] \end{cases} \quad (\text{A5})$$

$$x = 1 \rightarrow \begin{cases} p_+(1|1) = 1 - \exp \left[ -\frac{1+\alpha^2+\sqrt{2}\alpha}{2} \right] \\ p_-(1|1) = 1 - \exp \left[ -\frac{1+\alpha^2+\sqrt{2}\alpha}{2} \right] \end{cases} \quad (\text{A6})$$

$$x = 2 \rightarrow \begin{cases} p_+(1|2) = 1 - \exp \left[ -\frac{1+\alpha^2-\sqrt{2}\alpha}{2} \right] \\ p_-(1|2) = 1 - \exp \left[ -\frac{1+\alpha^2-\sqrt{2}\alpha}{2} \right] \end{cases} \quad (\text{A7})$$

$$x = 3 \rightarrow \begin{cases} p_+(1|3) = 1 - \exp \left[ -\frac{1+\alpha^2-\sqrt{2}\alpha}{2} \right] \\ p_-(1|3) = 1 - \exp \left[ -\frac{1+\alpha^2-\sqrt{2}\alpha}{2} \right] \end{cases} \quad (\text{A8})$$

From this table, we compute the maximum likelihood estimation for each combination of detection events, and the associated average probability of successful state discrimination:

$$p_s = \frac{1}{4} \left( 1 + 2 \exp \left[ -\frac{1+\alpha^2}{2} \right] \sinh \frac{\alpha}{\sqrt{2}} \right)^2. \quad (\text{A9})$$

This analytical result is essentially identical to the output of our numerical optimisation for small values of the amplitude  $\alpha$  ( $\alpha \lesssim 0.7$ ).